EC Journals.ASM.org

ERG2 and *ERG24* Are Required for Normal Vacuolar Physiology as Well as *Candida albicans* Pathogenicity in a Murine Model of Disseminated but Not Vaginal Candidiasis

Arturo Luna-Tapia,[a,b] Brian M. Peters,[b,c] Karen E. Eberle,[d] Morgan E. Kerns,[a] Timothy P. Foster,[a] Luis Marrero,[e] Mairi C. Noverr,[c] Paul L. Fidel, Jr.,[f] Glen E. Palmer[a,b]

Department of Microbiology, Immunology and Parasitology, School of Medicine, Louisiana State University Health Sciences Center, New Orleans, Louisiana, USA[a]; Department of Clinical Pharmacy, Division of Clinical and Experimental Therapeutics, College of Pharmacy, University of Tennessee Health Sciences Center, Memphis, Tennessee, USA[b]; Department of Prosthodontics, School of Dentistry, LSU Health Sciences Center, New Orleans, Louisiana, USA[c]; Department of Physiology, Louisiana State University Health Sciences Center, School of Medicine, New Orleans, Louisiana, USA[d]; Department of Medicine, Louisiana State University Health Sciences Center, School of Medicine, New Orleans, Louisiana, USA[e]; Department of Oral and Craniofacial Biology, School of Dentistry, LSU Health Sciences Center, New Orleans, Louisiana, USA[f]

Several important classes of antifungal agents, including the azoles, act by blocking ergosterol biosynthesis. It was recently reported that the azoles cause massive disruption of the fungal vacuole in the prevalent human pathogen *Candida albicans*. This is significant because normal vacuolar function is required to support *C. albicans* pathogenicity. This study examined the impact of the morpholine antifungals, which inhibit later steps of ergosterol biosynthesis, on *C. albicans* vacuolar integrity. It was found that overexpression of either the *ERG2* or *ERG24* gene, encoding C-8 sterol isomerase or C-14 sterol reductase, respectively, suppressed *C. albicans* sensitivity to the morpholines. In addition, both *erg2*Δ/Δ and *erg24*Δ/Δ mutants were hypersensitive to the morpholines. These data are consistent with the antifungal activity of the morpholines depending upon the simultaneous inhibition of both Erg2p and Erg24p. The vacuoles within both *erg2*Δ/Δ and *erg24*Δ/Δ *C. albicans* strains exhibited an aberrant morphology and accumulated large quantities of the weak base quinacrine, indicating enhanced vacuolar acidification compared with that of control strains. Both *erg* mutants exhibited significant defects in polarized hyphal growth and were avirulent in a mouse model of disseminated candidiasis. Surprisingly, in a mouse model of vaginal candidiasis, both mutants colonized mice at high levels and induced a pathogenic response similar to that with the controls. Thus, while targeting Erg2p or Erg24p alone could provide a potentially efficacious therapy for disseminated candidiasis, it may not be an effective strategy to treat vaginal infections. The potential value of drugs targeting these enzymes as adjunctive therapies is discussed.

A variety of antifungal therapies act by blocking the biosynthesis of the membrane lipid ergosterol (1). This includes the most important and widely used class of antifungal treatments, the azoles, which inhibit lanosterol demethylase (Erg11p) (2). The resulting depletion of cellular ergosterol and accumulation of intermediate sterol species are both thought to cause plasma membrane dysfunction and ultimately lead to growth arrest. However, we recently reported that inhibition of Erg11p also causes massive disruption of the fungal vacuole in the human pathogen *Candida albicans* (3). Furthermore, vacuolar fragmentation can be observed before significant growth inhibition and is thus an early consequence of azole treatment. Previous studies with the nonpathogenic yeast *Saccharomyces cerevisiae* also indicated that ergosterol is important for endocytic trafficking from the plasma membrane to the fungal vacuole (4) and to support homotypic vacuole-vacuole fusion in an *in vitro* biochemical assay (5). Several *S. cerevisiae* ergosterol biosynthetic mutants are known to have an aberrant vacuole morphology (5, 6), and it has been reported that the activity of the proton pump responsible for vacuolar acidification is also ergosterol dependent and therefore diminished in the presence of an azole antifungal (7). These findings are important, as it is known that defects in vacuolar biogenesis and/or acidification can have a significant impact upon fungal growth as well as *C. albicans* pathogenicity (8–13). Indeed, Zhang et al. suggested that defective vacuolar acidification may in part underlie the antifungal efficacy of the azoles (7); however, it is presently unknown if drugs that target alternative steps of the ergosterol biosynthetic pathway also affect vacuolar integrity or function. Intriguingly, *C. albicans* mutants blocked in various vacuolar trafficking pathways are hypersensitive to antifungal drugs that inhibit several distinct steps of ergosterol biosynthesis, including the azoles (14, 15), terbinafine, and the morpholines (3). This further supports a crucial interrelationship between vacuolar biogenesis, the sterol biosynthetic pathway, and the antifungal efficacy of ergosterol biosynthesis inhibitors.

The primary purpose of the present study was to examine how the morpholine antifungals affect the functional integrity of the

Received 27 July 2015 **Accepted** 29 July 2015

Accepted manuscript posted online 31 July 2015

Citation Luna-Tapia A, Peters BM, Eberle KE, Kerns ME, Foster TP, Marrero L, Noverr MC, Fidel PL, Jr, Palmer GE. 2015. *ERG2* and *ERG24* are required for normal vacuolar physiology as well as *Candida albicans* pathogenicity in a murine model of disseminated but not vaginal candidiasis. Eukaryot Cell 14:1006–1016. doi:10.1128/EC.00116-15.

Address correspondence to Glen E. Palmer, gpalmer5@uthsc.edu.

A.L.-T. and B.M.P. contributed equally to this article.

Supplemental material for this article may be found at http://dx.doi.org/10.1128/EC.00116-15.

doi:10.1128/EC.00116-15

fungal vacuole in the pathogenic yeast *C. albicans*. To achieve this, we focused on the *ERG2* and *ERG24* genes, which encode C-8 sterol isomerase and C-14 sterol reductase, respectively, as these are the proposed targets of the morpholines (16). The morpholines include the agriculturally important pesticides fenpropimorph and tridemorph. However, amorolfine is currently the only morpholine approved for medical use, as a topical treatment for fungal nail infections (1). We therefore concurrently examined the validity of targeting either Erg2p or Erg24p as a strategy to resolve either mucosal or disseminated candidiasis.

MATERIALS AND METHODS

Growth conditions. *C. albicans* was routinely grown on yeast extract-peptone-dextrose (YPD) agar plates at 30°C, supplemented with 50 μg ml^{-1} uridine when necessary. Selection of *C. albicans* transformants was carried out on minimal YNB medium (6.75 g $liter^{-1}$ yeast nitrogen base without amino acids, 2% dextrose, 2% Bacto agar) supplemented with the appropriate auxotrophic requirements described for *S. cerevisiae* (17) or with 50 μg ml^{-1} uridine. For growth curves, overnight cultures were subcultured into 20 ml fresh YPD or YNB broth to an optical density at 600 nm (OD_{600}) of 0.2 and then incubated at 30°C with shaking. The OD_{600} was determined from samples taken hourly.

Plasmid construction. Plasmid pLUX (18) was kindly provided by William Fonzi (Georgetown University). Plasmids pKE1 (19), pKE1-GFP-YPT72, and pKE1-CPP-GFP have been described previously (3). All oligonucleotides used in this study are listed in Table S1 in the supplemental material.

To construct the expression vector pKE3, 673 bp of the *C. albicans ENO1* promoter was amplified from strain SC5314 by use of primers ENO1prF2-KpnI and ENO1prR-SalI, digested with KpnI and SalI, and inserted between the same sites of pKE1 to replace the *ACT1* promoter. To facilitate overexpression, the *ERG1*, *ERG2*, *ERG11*, and *ERG24* open reading frames (ORFs) were amplified from SC5314 by using the ERG1ORFF/R, ERG2ORFF/R, ERG11ORFF/R, and ERG24ORFF/R primer pairs, respectively, and then each was cloned between the SalI and MluI sites of pKE3.

pLUX-ERG2 was made by PCR amplifying the *ERG2* ORF, along with 650 bp of the 5′-untranslated region (5′UTR) and 241 bp of the 3′UTR, from strain SC5314 by use of the primers ERG2AMPF and ERG2AMPR, digesting the product with KpnI and SacI, and then cloning it between the same sites of the pLUX vector. An identical strategy was used to clone the *ERG24* ORF, along with 760 bp of the 5′UTR and 379 bp of the 3′UTR, to form pLUX-ERG24. However, to facilitate the targeted integration of pLUX-ERG24 into the *URA3* loci of *C. albicans*, it was necessary to remove an NheI site internal to the *ERG24* ORF by site-directed mutagenesis. This was achieved by using a QuikChange kit (Promega) and the ERG24SDMF and ERG24SDMR primers. pKE1-UME6 was made by amplifying the *UME6* ORF with primers UME6ORFF and UME6ORFR and cloning the product downstream of the *ACT1* promoter, between the SalI and MluI sites of pKE1.

A *C. albicans* codon-adapted version of the Nano luciferase (Nluc) (20) coding sequence was produced with permission from Promega Corporation and synthesized by IDT DNA Technologies (see Table S2 in the supplemental material). To facilitate the expression of a cytoplasmic form of Nluc in *C. albicans*, the adapted Nluc coding sequence was amplified by PCR, using primers NLUCORFF-SalI and NLUCORFR-MluI, and cloned downstream of the *ACT1* promoter of pKE1, between SalI and MluI sites, to form pKE1-NLUC. To express a vacuole-targeted version of Nluc in *C. albicans*, the coding sequence of the predicted *C. albicans* Cpy1p prepropeptide (codons 1 to 129) (21) was amplified by PCR from SC5314 genomic DNA by using the primers CPPORFF-SalI and CPPORFR-EagI and then cloned between the SalI and EagI restriction sites of the pKE1 expression vector (19). The *C. albicans*-adapted Nluc coding sequence was then amplified by PCR, using primers NLUCORFF-EagI and NLUCORFR-MluI, and cloned in-frame and downstream of the *CPY1* prepropeptide coding sequence, between EagI and MluI sites, to yield the *CPY^{1-129}-NLUC* fusion construct pKE1-CPP-NLUC.

***C. albicans* strains.** SC5314 has been described previously (22), and CAI4 (23) was kindly provided by William Fonzi (Georgetown University). *C. albicans* was transformed with DNA constructs by using the lithium acetate procedure (24). Gene deletion strains were constructed by the PCR-based approach described by Wilson et al. (25), using the *ura3*Δ/Δ *his1*Δ/Δ *arg4*Δ/Δ strain BWP17 (kindly provided by Aaron Mitchell, Carnegie Mellon University). Gene deletion cassettes were amplified with primer set ERG2DISF/ERG2DISR or ERG24DISF/ERG24DISR, using pRSARG4ΔSpeI (*ARG4* marker) or pGEMHIS1 (*HIS1* marker) as the template. To make *erg2*Δ/Δ and *erg24*Δ/Δ single-gene deletion strains, alleles were sequentially replaced with the *HIS1* and *ARG4* selection markers. Correct integration of either gene deletion cassette was confirmed at each step by diagnostic PCR, using primers HIS1INTR and ERG2AMPR or ERG24AMPR to detect integration of the *HIS1* deletion cassette and primers ARG4INTR and ERG2AMPR or ERG24AMPR to detect integration of the *ARG4* deletion cassette. The absence of either the *ERG2* or *ERG24* open reading frame following deletion of both alleles was confirmed by PCR, using primer pair ERG2DETF/ERG2DETR or ERG24DETF/ERG24DETR, respectively. Finally, a "wild-type" copy of *ERG2* or *ERG24*, including 5′- and 3′-flanking sequences, was introduced into the respective gene deletion strains with pLUX-ERG2 or pLUX-ERG24 to produce prototrophic "reconstituted" strains. Isogenic gene deletion strains were produced by transforming the mutant strains with the pLUX vector alone. Each plasmid was digested with NheI to target integration into (and reconstitute) the *URA3* loci, circumventing the well-documented positional effects of *URA3* integration (26). Correct integration, and thus reconstitution, of the *URA3* loci was confirmed by the presence of a 2.2-kb product following PCR amplification with primers LUXINTDETF and LUXDETINTR.

The following expression vectors were all introduced into *ura3*$^-$ recipient strains following digestion with NheI: pKE1 (vector alone), pKE1-GFP-YPT72, pKE1-CPP-GFP, pKE1-NLUC, pKE1-CPP-NLUC, pKE1-UME6, pKE3 (vector alone), pKE3-ERG1, pKE3-ERG2, pKE3-ERG11, and pKE3-ERG24. Correct integration, and thus reconstitution, of the *URA3* loci was confirmed by PCR with primer pair LUXINTDETF/R as described above.

Antifungal susceptibility testing. The relative susceptibilities of *C. albicans* strains to various antifungal agents were tested on YPD agar plates supplemented with either 1 or 5 μg ml^{-1} fluconazole (Sigma-Aldrich), 0.05 or 0.01 μg ml^{-1} fenpropimorph, 0.01 or 0.0025 μg ml^{-1} amorolfine, 5 or 15 μg ml^{-1} tridemorph, 1 or 5 μg ml^{-1} terbinafine, or an equivalent volume of dimethyl sulfoxide (DMSO) solvent (no-drug control). Each *C. albicans* strain was grown overnight in YPD broth at 30°C, the cell density was adjusted to 10^7 ml^{-1} in sterile water, and serial 1:10 dilutions were performed in a 96-well plate. Cells were then applied to agar by use of a sterile multipronged applicator, incubated at 30°C, and imaged after either 24 or 48 h.

Stress phenotypes. *C. albicans* strains were grown overnight in YPD broth at 30°C, the cell density was adjusted to 10^7 ml^{-1} in sterile water, and serial 1:5 dilutions were performed in a 96-well plate. Cells were then applied to agar by use of a sterile multipronged applicator. Resistance to temperature stress was determined on YPD agar at 37 and 42°C; resistance to osmotic stress was determined on YPD agar plus 2.5 M glycerol; and resistance to ionic stress was determined on YPD plus 1 or 1.5 M NaCl and 100, 200, or 500 mM $CaCl_2$. Sensitivity to metal ion stress was also tested on YPD agar supplemented with 50 μM $CuCl_2$, 50 μM $ZnCl_2$, and 10 mM $MnCl_2$. Xenobiotic stresses included YPD agar plates supplemented with 1 nM rapamycin, 5 mM sodium vanadate, and 5 mM caffeine. Cell surface defects were examined on YPD agar plus 50 μg ml^{-1} Congo red or 0.02% SDS. The ability to utilize nonfermentable carbon sources was tested on YPG agar (YPD agar with 3% glycerol in place of dextrose). Growth rates of mutant and control strains were also compared on unbuffered YNB agar as well as YNB agar buffered with 0.3 M MOPS (morpholinepropane-

sulfonic acid) and pH adjusted to either 5.5, 7, or 8.5. Secreted protease activity was examined on bovine serum albumin (BSA)-yeast extract (YE) agar at 37°C (27). Sensitivity to H_2O_2 was determined in a 96-well plate-based assay by examining growth in YPD medium supplemented with 0 to 12 mM H_2O_2 after 24 h of incubation at 30°C.

Morphogenesis assays. Filamentous growth was assessed on M199 medium (pH 7.5) and 10% fetal bovine serum (FBS) agar (28). Hyphal growth was also induced in liquid M199 or 10% FBS medium at 37°C, following inoculation of yeast at 10^6 cells ml^{-1}. After 180 min, samples were taken, immediately fixed with formalin, and examined microscopically. Filamentous growth was also stimulated by sandwiching *C. albicans* cells between two layers of YPS agar (29). *UME6*-overexpressing strains were streaked onto YPD agar plates and incubated at 30°C, and colony morphologies were compared after 24 and 48 h.

Fluorescence microscopy to determine vacuole morphology. Vacuole morphology was determined using *C. albicans* strains expressing either the green fluorescent protein (GFP)-Ypt72p (8) or $Cpy1^{1–129}$-GFP fusion protein. In some experiments, cells were prelabeled with the dye FM4-64 to label the vacuolar membrane, as previously described (30). To examine the effects of the morpholine compounds on vacuolar integrity, a GFP-Ypt72p-expressing strain was grown overnight in YNB broth at 30°C and then subcultured at 10^6 cells ml^{-1} into fresh YNB supplemented with either 1.56 μg ml^{-1} amorolfine, 2 μg ml^{-1} fenpropimorph, 2 μg ml^{-1} tridemorph, or 0.5% DMSO (drug-free control). After incubation at 30°C for 6 h, cells were observed with a fluorescence microscope, using a 100× objective and a fluorescein isothiocyanate (FITC) filter set to detect GFP fluorescence. Where appropriate, a tetramethyl rhodamine isocyanate (TRITC) filter set was also used to observe FM4-64. Matching phase-contrast and fluorescence images were acquired for each field. Where adjustments in the brightness and/or contrast of images were made, all images presented for a given time point/condition in each experiment were scaled identically to permit direct comparisons. Manders colocalization coefficients were calculated using ImageJ software.

Quinacrine accumulation assay. Labeling of the *C. albicans* vacuole with quinacrine was performed based on the method described by Baggett et al. (31), with the following modifications. Quinacrine stocks (10 mM) were prepared in 1 M HEPES, pH 7.6. Cells were grown overnight in YPD broth at 30°C. Approximately 5×10^7 cells of each strain were harvested in each of three microcentrifuge tubes (to provide triplicate measurements for each sample) and resuspended in 100 μl of assay buffer (100 mM HEPES plus 2% glucose). Quinacrine was added to each sample, to a final concentration of 25 μM; three identical samples in the absence of quinacrine were prepared for each strain to measure cell autofluorescence. A no-cell control containing assay buffer and 25 μM quinacrine was also included. Samples were incubated for 5 min at room temperature in the dark and then pelleted in a microcentrifuge for 30 s, and the cells were then resuspended in 100 μl of fresh assay buffer without quinacrine and placed on ice. One hundred microliters of each sample was then transferred to a black, flat-bottom 96-well plate. Fluorescence intensity (excitation, 490 nm; emission, 525 nm; 9-nm bandwidth) was then measured using a Cytation 5 Multi-Mode reader (BioTek). Background fluorescence from unlabeled cells and medium was subtracted, and the fluorescence intensity was normalized to the OD_{600} of each sample and expressed in relative fluorescence units (RFU).

Mouse model of vaginal candidiasis. The animals used in this study were housed in AAALAC-approved facilities located at the School of Dentistry, LSU Health Sciences Center (LSUHSC). The LSUHSC Animal Care and Use Committee approved all animal use and protocols. Mice were given standard rodent chow and water *ad libitum*. Mice were monitored daily for signs of distress, including noticeable weight loss and lethargy. The murine model of *Candida* vaginitis has been reported extensively in the literature and was performed as described previously (32). C57BL/6 mice were purchased from The Jackson Laboratory and housed in isolator cages mounted onto ventilated racks. Mice were administered 0.1 mg of estrogen (β-estradiol 17-valerate; Sigma) dissolved in 0.1 ml of sesame oil subcutaneously 72 h prior to inoculation with *C. albicans*. Estrogen injections were administered weekly thereafter. Stationary-phase cultures of *C. albicans* isolates were washed three times in sterile, endotoxin-free phosphate-buffered saline (PBS) and resuspended in a 0.2× volume of PBS. Cell suspensions were diluted, counted on a Neubauer hemocytometer, and adjusted to 2.5×10^8 CFU ml^{-1} in sterile PBS. Estrogen-treated mice were inoculated intravaginally with 20 μl of the standardized cell suspension, generating an inoculum size of 5×10^6 blastoconidia. All animal experiments were conducted in duplicate, with 4 mice per group; all reported data are cumulative ($n = 8$) for these independent experiments.

Analysis of vaginal lavage fluid. Groups of mice were briefly anesthetized by isoflurane administration and underwent vaginal lavage with 100 μl PBS at days 7 and 10 postinoculation (p.i.). Recovered lavage fluids were kept on ice during processing. Lavage fluids were assayed for fungal burdens by making 10-fold serial dilutions in sterile PBS and plating the dilutions on YPD agar containing 50 μg ml^{-1} chloramphenicol to inhibit bacterial overgrowth, using the drop-plate method as described previously (33). Plates were allowed to dry and then incubated for 24 h at 37°C, and the resulting colonies were enumerated. The median number of CFU per milliliter per group is reported. Polymorphonuclear leukocytes (PMNs) in the vaginal lavage fluid were quantified by standard light microscopy, using the Papanicolaou staining technique ("Pap smear") as described previously (32). PMN counts were averaged per field and are reported as the mean PMN count per group ± the standard error of the mean (SEM).

Mouse model of hematogenously disseminated candidiasis. All procedures were approved by the Institutional Animal Care and Usage Committee of LSUHSC-New Orleans and complied with all relevant federal guidelines. *C. albicans* was grown overnight in YPD cultures at 30°C (200 rpm). Cells were washed twice in sterile PBS, and cell density was determined using a hemocytometer. Each strain was then diluted to 5×10^6 cells ml^{-1} in sterile PBS. Each cell suspension (0.1 ml) was then inoculated into the lateral tail vein of BALB/c mice. Viable cell counts of each inoculum were confirmed by plating appropriate dilutions onto YPD agar plates and counting the number of colonies formed after 48 h. Mice were monitored for 14 days, and those showing distress were euthanized. Kaplan-Meier survival curves were plotted, and statistical significance was determined using the log rank test. Surviving mice were euthanized on day 14 postinoculation. The kidneys from each mouse were weighed and homogenized in PBS, and serial dilutions of the homogenates were plated on YPD agar. The number of colonies on each plate was counted after 48 h, and the number of CFU per gram of tissue was calculated.

Luciferase assays. *C. albicans* strains expressing either Nluc or the $Cpy^{1–129}$-Nluc fusion protein were cultured overnight in YPD broth at 30°C. Two hundred microliters of each culture was then transferred to an Eppendorf tube, and the cells were pelleted using a microcentrifuge. The culture supernatant was then removed, and the cells were resuspended in 1 ml YNB broth and then further diluted 1:100 in YNB medium. Two hundred microliters of each cell suspension was then dispensed into the wells of a round-bottom 96-well plate. After 24 h of incubation in a 30°C standing incubator, the cells in each well were resuspended by mixing using a multichannel pipette. The plates were then centrifuged at 1,200 rpm in a benchtop centrifuge to pellet the cells. Fifty microliters of the culture supernatant was then transferred to a fresh, flat-bottom 96-well plate, and the amount of Nluc activity was determined using the Nano-Glo luciferase assay reagent (Promega Corporation) per the manufacturer's instructions. Luminescence in each well was then measured by using a BioTek Synergy MX plate reader. Growth in each well from the overnight incubation was also determined by measuring the OD_{600} of samples diluted 1:10 in distilled water, using a separate flat-bottom 96-well plate, and each luminescence reading was normalized to the corresponding OD_{600} reading.

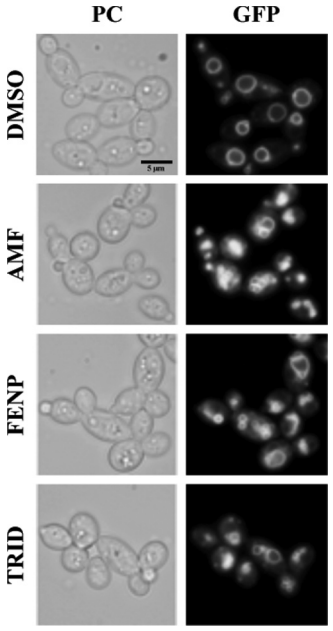

FIG 1 The morpholine antifungals cause disruption of the *C. albicans* vacuole. A GFP-Ypt72p-expressing strain of *C. albicans* was grown in YNB medium supplemented with either 1.56 μg ml^{-1} amorolfine (AMF), 2 μg ml^{-1} fenpropimorph (FENP), 2 μg ml^{-1} trimedorph (TRID), or an equivalent amount of DMSO (0.5%; no-drug control) at 30°C. After 6 h, vacuolar morphology was examined using a fluorescence microscope. GFP images were acquired with an FITC filter set. PC, phase-contrast images.

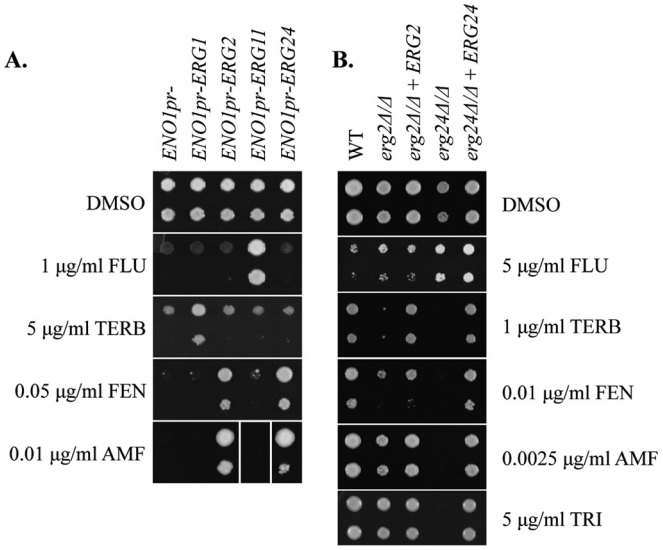

FIG 2 Erg2p and Erg24p expression affects *C. albicans* susceptibility to the morpholine antifungals. (A) The *ERG1*, *ERG2*, *ERG11*, and *ERG24* ORFs were each overexpressed from the *ENO1* promoter in *C. albicans* strain CAI4. Isolates of each genotype were suspended at 10^7 cells ml^{-1} (top rows) and 10^6 cells ml^{-1} (bottom rows) and placed as spots on YPD agar enriched with the indicated antifungal agents or with an equivalent amount of DMSO solvent. The plates were then imaged after 24 h (DMSO) or 48 h (all other plates). (B) The susceptibility of the *C. albicans erg2*Δ/Δ and *erg24*Δ/Δ mutants, their isogenic revertant strains, and the clinical isolate SC5314 (wild type [WT]) to the indicated antifungal agents was tested as described above. FLU, fluconazole; TERB, terbinafine.

RESULTS

The morpholine antifungals cause significant vacuolar disruption in *C. albicans*. Given the severe vacuolar defects we previously observed following azole-mediated inhibition of Erg11p (3), we examined if blocking ergosterol biosynthesis with the morpholine antifungals would also disrupt vacuolar integrity. This was conducted using a *C. albicans* strain expressing a GFP-Ypt72p fusion protein (8). Ypt72p is a Rab GTPase that inserts into the outer leaflet of the vacuolar membrane via a lipid-modified C terminus. When cultured in the presence of either amorolfine, fenpropimorph, or tridemorph, cells exhibit a highly fragmented vacuolar structure (Fig. 1) similar to that previously described for culture with fluconazole (3).

***C. albicans erg2*Δ/Δ and *erg24*Δ/Δ mutants have defective vacuolar morphology.** The morpholines are reported to inhibit both C-8 sterol isomerase (Erg2p) and C-14 sterol reductase (Erg24p) (16). This is supported by the fact that overexpression of either *ERG2* or *ERG24* reduced *C. albicans* susceptibility to both amorolfine and fenpropimorph (Fig. 2A) but not to fluconazole or terbinafine. In contrast to a previous report (34), we found that the *C. albicans erg24*Δ/Δ mutant was hypersensitive to amorolfine, fenpropimorph, and tridemorph (Fig. 2B), while the *erg2*Δ/Δ mutant was also sensitive to fenpropimorph. Our results are consistent with the finding that the loss of both *ERG2* and *ERG24* results in a synthetic lethal phenotype in *S. cerevisiae* (35). This pattern of susceptibility also reflects the preferential inhibition of Erg2p over Erg24p by the morpholines, with the exception of fenpropimorph (34, 36). In agreement with the previous study, we found that both the *erg2*Δ/Δ and *erg24*Δ/Δ mutants were highly sensitive to terbinafine (Fig. 2B). We also noted that the *erg2*Δ/Δ mutant was 2-fold more resistant to amphotericin B, while both mutants were 2- to 4-fold more resistant to caspofungin than their isogenic control strains (see Fig. S1 in the supplemental material).

In order to determine if the vacuolar defects observed in the presence of the morpholines were the result of Erg2p and/or Erg24p inhibition, we examined vacuolar integrity in the *erg2*Δ/Δ and *erg24*Δ/Δ mutants by using GFP-Ypt72p. Each strain was colabeled with FM4-64, a lipophilic dye that binds to the plasma membrane and is internalized via endocytosis to label the vacuolar membrane (30). This revealed that while many of the *erg2*Δ/Δ mutant cells had apparently normal spherical vacuoles, about half of the cells had a multilamellar or densely clustered vacuolar structure not observed in the wild-type control (Fig. 3). The defects were similar but more severe in the *erg24*Δ/Δ mutant. Furthermore, while GFP-Ypt72p was tightly associated with the FM4-64-labeled vacuolar membrane in the control strain, this association was slightly less avid in the *erg2*Δ/Δ and *erg24*Δ/Δ mutants. While the vacuolar fragmentation observed in these mutants resembled that in the presence of the morpholines, it was also somewhat less severe. This may suggest that simultaneous inhibition of both Erg2p and Erg24p exacerbates the vacuolar defects.

***erg2*Δ/Δ and *erg24*Δ/Δ mutants share several stress phenotypes with vacuole-deficient mutants.** Mutants deficient in vacuolar biogenesis or acidification exhibit a characteristic set of stress phenotypes, including sensitivity to osmotic, ionic, and pH stresses (37). We therefore tested the two *erg* mutants for a variety of stress phenotypes that have been associated with vacuolar dysfunction. *C. albicans* mutants with severe defects in vacuole biogenesis have significantly reduced growth rates and are sensitive to an elevated growth temperature (38). While both *erg2*Δ/Δ and

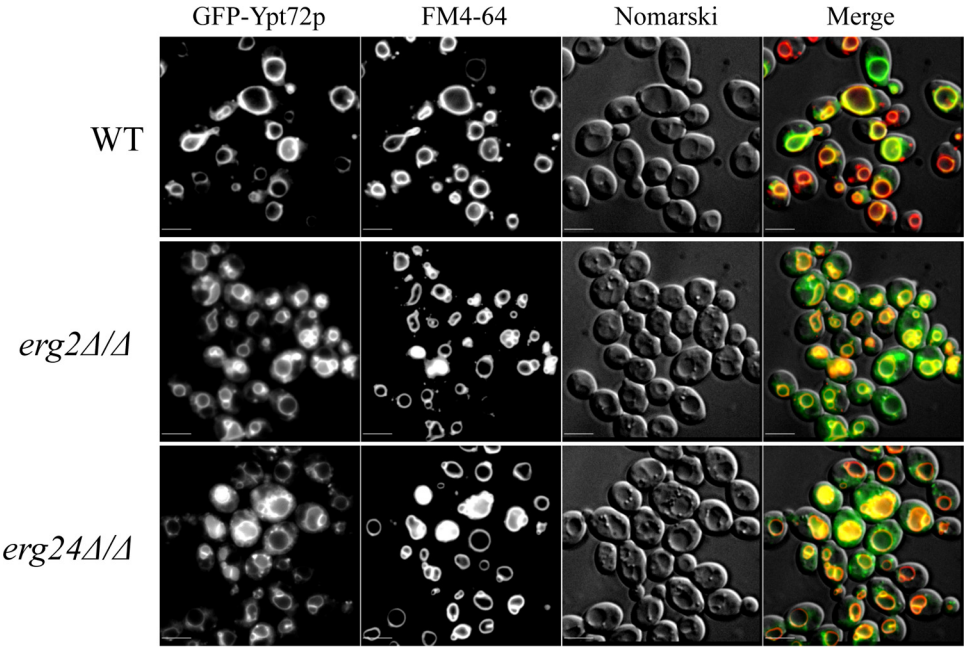

FIG 3 *C. albicans erg2*Δ/Δ and *erg24*Δ/Δ mutants have an abnormal vacuole morphology. The *GFP-YPT72* expression construct was introduced into the *C. albicans erg2*Δ/Δ and *erg24*Δ/Δ mutants and the control strain CAI4. Each strain was then pulse-chase labeled with FM4-64, and cells were observed using a fluorescence microscope. For the merged images (right side), red shows FM4-64 staining, and green shows GFP staining. Bars = 5 μm. Colocalization coefficients for GFP colocalizing with FM4-64 were as follows: for the WT, 0.890 ± 0.027; for the *erg2*Δ/Δ mutant, 0.683 ± 0.049; and for the *erg24*Δ/Δ mutant, 0.748 ± 0.046 ($n = 3$ fields of view).

*erg24*Δ/Δ mutant strains were viable, it was immediately apparent that the *erg24*Δ/Δ mutant had a growth defect under routine culture conditions, as reported previously (34). In YPD broth at 30°C, both the *erg2*Δ/Δ and *erg24*Δ/Δ mutants had reduced growth rates as determined by the OD_{600} (see Fig. S2 in the supplemental material). Both mutants were also sensitive to growth with high concentrations of ionic or osmotically active substances, such as NaCl and glycerol (Fig. 4A), with the *erg24*Δ/Δ mutant being affected more severely than the *erg2*Δ/Δ mutant.

Ergosterol is reported to be required to support the activity of the V-ATPase H^+ pump responsible for vacuolar acidification (7). Loss of V-ATPase activity is associated with a specific set of phenotypes, including reduced growth at or above pH 7, sensitivity to elevated concentrations of calcium and other metal ions, including zinc, an inability to utilize nonfermentable carbon sources, and hypersensitivity to oxidative stress (39). Both *erg* mutants were less tolerant of alkaline growth conditions than the control strains (Fig. 4B) and were also less tolerant of elevated levels of manganese chloride. However, the *erg* mutants were not sensitive to zinc chloride, were able to grow on the nonfermentable carbon source glycerol, and were not sensitive to H_2O_2-induced oxidative stress (data not shown). Interestingly, the addition of 100 mM $CaCl_2$ to YPD agar plates seemed to inhibit the growth of both *erg* mutants. Paradoxically, and in contrast to what was previously reported by Jia et al. (34), the addition of higher concentrations of $CaCl_2$ ameliorated this phenotype. Thus, the *C. albicans erg2*Δ/Δ and *erg24*Δ/Δ mutants did not exhibit the full complement of phenotypes characteristic of mutants deficient in V-ATPase activity. In addition, both *erg* mutants actually accumulated larger quantities of the weak base quinacrine within their vacuoles than that in the wild-type control strain (Fig. 4C; see Fig. S3 in the supplemental material). Quinacrine freely passes through cellular membranes by passive diffusion, but it becomes protonated within acidic cellular compartments, enhancing its fluorescence and reducing its ability to permeate the membrane (31). Thus, quinacrine accumulates within acidic compartments, primarily the fungal vacuole. As such, our data imply that both the *erg2*Δ/Δ and *erg24*Δ/Δ mutants have a more acidic vacuolar lumen than that of the control strains and that the V-ATPase function must thus be intact.

The *erg24*Δ/Δ mutant and, to a lesser extent, the *erg2*Δ/Δ mutant were sensitive to the cell wall binding agent Congo red, and both were extremely sensitive to the detergent SDS, indicating significant defects in cell wall composition and cell membrane integrity, respectively. While these phenotypes are expected for strains depleted of membrane ergosterol, they have also been observed for some vacuolar trafficking mutants (9). Collectively, these results indicate a substantial but incomplete overlap between the stress tolerance phenotypes of the *erg2*Δ/Δ and *erg24*Δ/Δ mutants and those observed for vacuole-deficient *C. albicans* mutants.

***C. albicans erg2*Δ/Δ and *erg24*Δ/Δ mutants do not missort vacuolar carboxypeptidase Y.** Abnormal vacuolar morphology can arise as a secondary consequence of membrane trafficking defects from the Golgi apparatus to the vacuole (40). To determine how Golgi-vacuole trafficking is affected in the *erg2*Δ/Δ and *erg24*Δ/Δ mutants, we examined the localization of a Cpy1-GFP fusion protein (3). In *S. cerevisiae*, Cpy1p (carboxypeptidase Y) is synthesized with an N-terminal prepropeptide that directs its entry into the secretory network at the endoplasmic reticulum and its subsequent sorting to the vacuole via the Golgi apparatus and the late endosome (41, 42). We therefore introduced a fusion be-

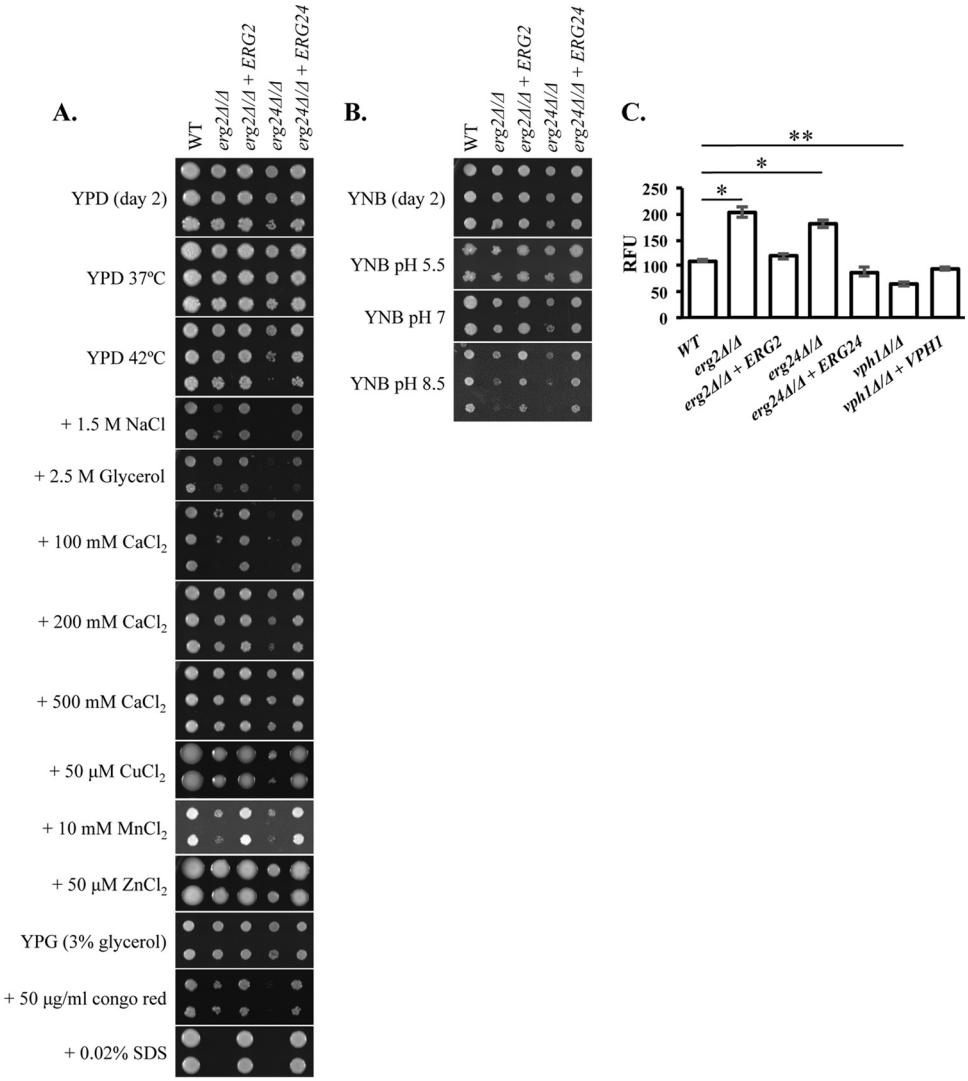

FIG 4 The *C. albicans erg2*Δ/Δ and *erg24*Δ/Δ mutants exhibit a subset of stress phenotypes characteristic of vacuole-deficient mutants. (A) Cell suspensions of the *C. albicans* mutant and control strains were prepared by serial dilution and then applied to YPD agar or YPD agar supplemented with the indicated compounds. Each agar plate was incubated at 30°C (except for the 37°C and 42°C plates indicated) and imaged after 48 h. The 2.5 M glycerol plate was imaged after 72 h. (B) Each strain was applied to YNB agar plates adjusted to the indicated pH, incubated at 30°C, and imaged after 48 h. (C) Intracellular accumulations of quinacrine were compared for the indicated *C. albicans* strains, using a 96-well plate-based assay. Following incubation in the presence of 25 μM quinacrine, relative fluorescence was measured by using an excitation wavelength of 490 nm and an emission wavelength of 525 nm. Background fluorescence was determined for each strain by using identically treated cells in the absence of quinacrine and was subtracted to calculate the quinacrine-specific fluorescence. The *vph1*Δ/Δ mutant was included as a control, as it lacks the vacuole-specific isoform of the V-ATPase subunit a. Each bar indicates the relative fluorescence for each strain, as the average for two independent experiments. Error bars indicate standard deviations. *, $P < 0.05$; **, $P < 0.01$. WT, strain SC5314.

tween the predicted prepropeptide coding sequence of *C. albicans CPY1* and the GFP gene (*CPY1*$^{1–129}$*-GFP*) (3) into mutant and control strains. Microscopic examination revealed that the majority of the GFP fusion was localized within the lumen of the FM4-64-labeled vacuoles in both control and mutant strains, and thus no gross defects in Cpy1$^{1–129}$-GFP transport were apparent (see Fig. S4 in the supplemental material). In order to detect more subtle defects in vacuolar trafficking, we used a second, more sensitive reporter of Golgi-vacuole trafficking. In *Saccharomyces*, perturbation of Golgi-vacuole trafficking leads to missorting of a portion of Cpy1p into the secretory pathway, and Cpy1p activity can thus be detected within the culture supernatant (43, 44). To detect Cpy1p missorting in *C. albicans*, we fused the *C. albicans CPY1* prepropeptide coding sequence with a *C. albicans*-adapted Nano luciferase (Nluc; Promega Corporation) coding sequence. Nluc is reported to be over 100-fold brighter than other naturally occurring luciferase enzymes (20) and is therefore an extremely sensitive reporter. The *CPY1*$^{1–129}$*-NLUC* expression construct was introduced into both *erg* mutants as well as a wild-type control strain, and the levels of Nluc activity in the cell-free culture supernatants were compared. Significantly more Cpy1$^{1–129}$-Nluc activity was released into the culture supernatant by both *erg* mutants than by the wild-type control (Fig. 5A). However, this differential was even more dramatic when a cytoplasmic form of Nluc was expressed (Fig. 5B), suggesting that the release of Cpy1$^{1–129}$-Nluc is most likely a secondary consequence of cell lysis or increased

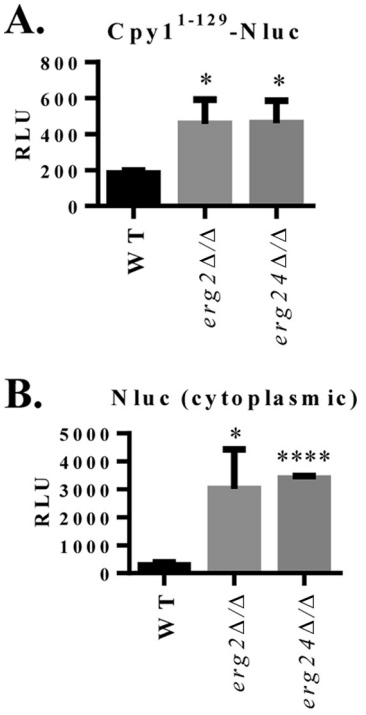

FIG 5 Vacuolar carboxypeptidase Y is not missorted in *C. albicans erg2*Δ/Δ and *erg24*Δ/Δ mutants. (A) The predicted Cpy1p prepropeptide was fused to Nluc, and the resulting expression construct was introduced into the *erg2*Δ/Δ, *erg24*Δ/Δ, and wild-type (CAI4) strains. Each strain was then grown in YNB medium within 96-well plates, and the amount of $Cpy1^{1-129}$-Nluc missorting into the culture supernatant was quantified. (B) To control for Nluc that may be released due to cell lysis or leakage across the plasma membrane, an equivalent construct expressing Nluc alone (cytoplasmic) was introduced into each strain, and Nluc release was determined as described above. Each bar and error bar indicates the mean and standard deviation for four separate isolates of each genotype. RLU, relative light units. To determine if the Nluc release from each mutant was significantly different from that of the WT, data were compared using the unpaired two-tailed *t* test with Welch's correction. *, $P < 0.05$; ****, $P < 0.0001$.

membrane permeability rather than a specific vacuolar trafficking defect.

***erg2*Δ/Δ and *erg24*Δ/Δ mutants have severe defects in hyphal growth.** During the transition from yeast to hyphal growth, the fungal vacuole undergoes a rapid and dynamic expansion to fill the subapical regions of the emerging germ tube (45, 46). Furthermore, a number of *C. albicans* mutants with abnormal vacuoles are unable to form true hyphae. This is important because hyphal growth has been shown to make a major contribution to *C. albicans* pathogenicity (47, 48). We therefore tested the ability of the *erg2*Δ/Δ and *erg24*Δ/Δ mutants to form hyphae under a variety of conditions, including on 10% FBS and M199 agar (Fig. 6A; see Fig. S5A in the supplemental material), as well as within YPS agar "sandwich" cultures (see Fig. S5B). Neither mutant was able to produce significant filamentous growth under any of these conditions. We also compared the morphological forms produced at the cellular level following induction of hyphal growth in either liquid M199 or 10% FBS medium (Fig. 6B). Again, both the *erg2*Δ/Δ and *erg24*Δ/Δ mutants had severe deficiencies in hyphal formation, with both mutants forming only short germ tubes, many of which appeared to revert to a budding mode of growth (yeast) from the hyphal tip. As viewed with the GFP-Ypt72p fusion protein, the vacuole morphology appeared to be highly fragmented in the *erg2*Δ/Δ germ tubes as well as the parental yeast cells. In contrast, while only small GFP-labeled compartments were observed in the *erg24*Δ/Δ germ tubes, large spherical vacuoles could be observed in the parent yeast cells. This suggested that neither the *erg2*Δ/Δ nor *erg24*Δ/Δ mutant was able to support the formation of the large tubular vacuoles normally observed in elongating *C. albicans* hyphae. Finally, we attempted to "force" hyphal growth through the overexpression of Ume6p, a transcription factor that activates and sustains hyphal growth (49). However, Ume6p overexpression was not sufficient to suppress the hyphal growth defects of the *erg2*Δ/Δ and *erg24*Δ/Δ mutants (see Fig. S5C).

***erg2*Δ/Δ and *erg24*Δ/Δ mutants are pathogenic in a mouse model of vaginal but not disseminated candidiasis.** Finally, we examined the pathogenicity of the *erg2*Δ/Δ and *erg24*Δ/Δ mutants in a mouse model of vaginal candidiasis. Surprisingly, both mu-

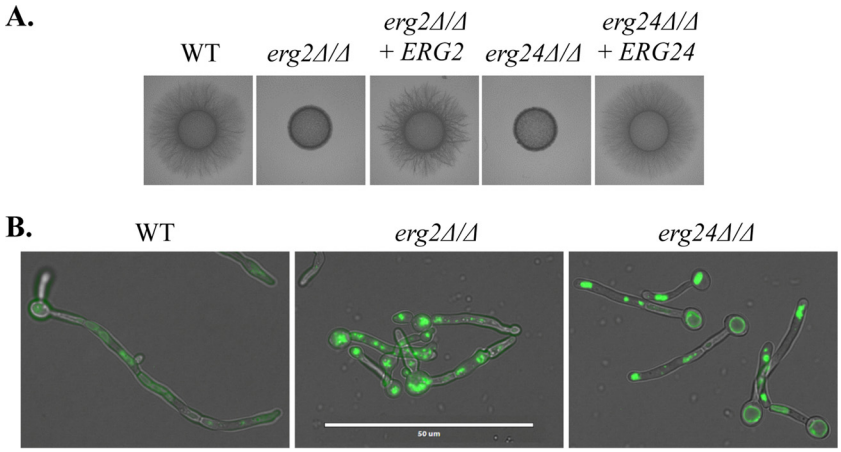

FIG 6 *C. albicans erg2*Δ/Δ and *erg24*Δ/Δ mutants have significant defects in polarized hyphal growth. (A) Cell suspensions of each strain were applied to 10% FBS agar plates and incubated at 37°C for 4 days. (B) WT, *erg2*Δ/Δ, and *erg24*Δ/Δ strains expressing the GFP-Ypt72p fusion were induced to form hyphae in M199 medium at 37°C for 3 h and then imaged using a fluorescence microscope (60×). Merged bright-field and FITC images are shown.

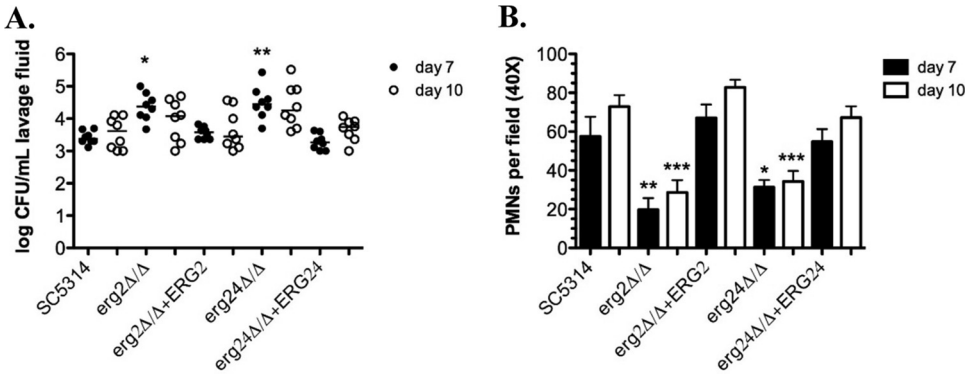

FIG 7 *C. albicans erg2*Δ/Δ and *erg24*Δ/Δ mutants efficiently colonize mice in a mouse model of vaginal candidiasis. C57BL/6 mice were treated with estrogen, inoculated with 5×10^6 CFU of each *C. albicans* strain, and subjected to vaginal lavage at days 7 and 10 postinoculation. Lavage fluids were assessed for fungal burdens by standard microbiological plating (medians) (A), and PMNs were examined by Pap staining (means and SEM) (B). All data are cumulative from two independent experiments ($n = 4$ per group; 8 mice total). For microbial burdens, statistical analysis of significance was performed by using Kruskal-Wallis one-way analysis of variance (ANOVA) with Dunn's multiple-comparison posttest. For PMN data, statistical analysis was performed by using one-way ANOVA and Dunnett's multiple-comparison posttest. Significance is denoted as follows: *, $P < 0.05$; **, $P < 0.01$; and ***, $P < 0.001$.

tant strains colonized the mice at higher densities than those of the control strains, as determined by CFU counts (Fig. 7A). In addition, both mutants induced the characteristic PMN infiltration that has been associated with symptomatology, albeit at lower levels than those with the control strains (Fig. 7B) (50). Because PMN infiltration has been associated with *C. albicans* hyphal formation (32), we examined the cellular morphology of each strain from fixed aliquots of the lavage fluid. Hyphal elements could be discerned in the vaginal lavage fluid of mice infected with either deletion mutant (see Fig. S6 in the supplemental material); however, these were typically much shorter than those of the control strains.

The proficiency of the *erg2*Δ/Δ and *erg24*Δ/Δ mutants at colonizing the mouse vagina was unexpected given the severe growth, stress tolerance, and hyphal growth defects described above. In addition, a previous study determined that a *C. albicans erg24*Δ/Δ mutant had substantially diminished virulence in a mouse model of disseminated infection (34). We therefore examined the virulence of our *erg2*Δ/Δ and *erg24*Δ/Δ mutants in the mouse model of disseminated candidiasis. All mice infected with the mutant strains survived the duration of the experiment (14 days), while those infected with the control strains succumbed by day 8 (Fig. 8). Furthermore, the fungal burdens within the kidneys of the surviving mice were below the level of detection for 2 of the 5 *erg2*Δ/Δ mutant-infected mice and 3 of the 5 *erg24*Δ/Δ mutant-infected mice, and only very low levels of colonization were detected in the remaining animals. This confirms that both mutants are essentially avirulent in the disseminated model of candidiasis.

DISCUSSION

Vacuoles are typically thought to have a very low ergosterol content compared to the plasma membrane (51, 52), yet several lines of evidence suggest that interfering with fungal sterol metabolism can have a profound impact upon the function of this organelle (5–7). We recently reported that the azole-mediated inhibition of Erg11p caused massive disruption of the *C. albicans* vacuole. Here we extended that finding by showing that inhibition of the later steps of the ergosterol biosynthetic pathway by use of the morpholine class of antifungal drugs also causes substantial defects in vacuolar integrity.

Providing further evidence that the morpholine antifungals target both Erg2p and Erg24p in *C. albicans*, we found that overexpression of either protein could enhance *C. albicans* resistance to this class of compound. This result contrasts with the case for *S. cerevisiae*, in which overexpression of *ERG24*, but not *ERG2*, suppresses morpholine antifungal activity (53). This may reflect a difference in the propensity of the morpholines to target the Erg2p and Erg24p enzymes of either species. In addition, we also found that a *C. albicans erg24*Δ/Δ mutant is highly susceptible to fenpropimorph, amorolfine, and tridemorph. This conflicts with the previous report of Jia et al. (34), whose *erg24*Δ/Δ mutant was more resistant to morpholines than their control strain. One possible explanation for this discrepancy is the different nutritional requirements of the mutant versus control strains used in that study, whereas all of our strains were prototrophic. This is potentially significant, as it has been established for *S. cerevisiae* that ergosterol availability influences the trafficking, and thus activity, of various nutrient transporters at the cell surface, including uracil permease and a general amino acid transporter (54, 55). Thus, the

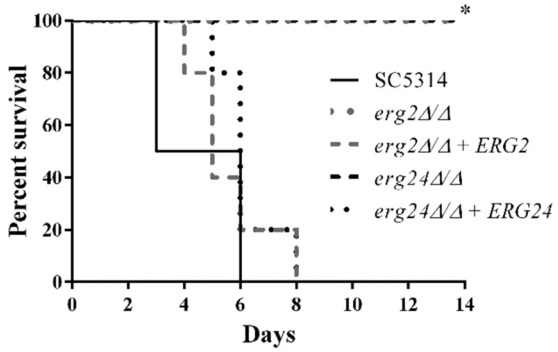

FIG 8 *C. albicans erg2*Δ/Δ and *erg24*Δ/Δ mutants are avirulent in a mouse model of disseminated candidiasis. Five BALB/c mice were inoculated intravenously with approximately 5×10^5 yeast cells of each *C. albicans* strain. Survival curves were plotted for a 14-day period. This experiment was conducted only once, as the results are consistent with those previously reported by Jia et al. (34). To determine the statistical significance of the different survival rates, the data sets for the groups of mice were compared to those for the SC5314 control group by using the log rank test. *, $P = 0.0039$.

consequences of inhibiting ergosterol biosynthesis may be exacerbated in strains with deficiencies in metabolite biosynthesis, such as the BWP17 control strain used in the study of Jia et al.

In *S. cerevisiae*, the loss of both *ERG2* and *ERG24* leads to a synthetic lethal phenotype (35). Thus, our data are consistent with fenpropimorph acting upon both Erg2p and Erg24p, as the loss of either renders *C. albicans* hypersensitive to this agent. In contrast, we found that loss of *ERG24*, but not *ERG2*, leads to *C. albicans* hypersusceptibility to tridemorph and amorolfine, which supports previous evidence that tridemorph preferentially targets Erg2p over Erg24p (34, 36). Although ergosterol biosynthesis is often viewed as a linear pathway, with Erg2p acting several steps downstream of Erg24p, collectively these data suggest that inhibiting multiple steps can lead to synergistic antifungal activity. Furthermore, the simplistic view of sterol biosynthesis as a linear sequence of biochemical reactions catalyzed by a specific order of enzymes grossly underrepresents the complexity of this pathway and may underestimate its potential for therapeutic exploitation.

Through deletion of either the *ERG2* or *ERG24* gene, we were able to determine how blocking either step in sterol biosynthesis affects vacuolar function in *C. albicans*. While both the *erg2*Δ/Δ and *erg24*Δ/Δ mutants have an abnormal vacuolar morphology, neither exhibits the strong *vma* phenotype characteristic of mutants defective in vacuolar acidification. Furthermore, both mutants hyperaccumulate the base quinacrine within the vacuole lumen, indicating a highly acidified vacuole. This could indicate that the V-ATPase proton pump is hyperactive in these mutants, and deregulation of V-ATPase activity could account for their inability to grow under alkaline conditions. Alternatively, increased vacuolar acidification could result from reduced activity of the H^+-dependent transporters that facilitate the sequestration of various metabolites and toxic substances within the vacuole (56). This could account for the mutant's hypersensitivity to various metal ions and xenobiotics. Either way, these data indicate that the function or regulation of at least a subset of vacuolar membrane proteins is affected by its sterol composition.

During the course of this work, we noted that both the *erg2*Δ/Δ and *erg24*Δ/Δ *C. albicans* mutants had substantially less secreted protease activity *in vitro* than their isogenic controls (see Fig. S7 in the supplemental material), yet both mutants successfully exported a large quantity of a secreted form of the Nluc luciferase protein (unpublished results), demonstrating that they are secretion competent. One possible explanation for this apparent paradox is that the secreted aspartyl proteases of *C. albicans* are transported from the Golgi apparatus to the cell surface via the late endosomal prevacuolar compartment (PVC) (57), whereas the secreted luciferase is more likely transported directly from the Golgi apparatus to the cell surface. Thus, it is possible that the prevacuolar secretory pathway is selectively affected in the *erg2*Δ/Δ and *erg24*Δ/Δ mutants. Furthermore, the transport of vacuolar Cpy1p, which also occurs from the Golgi apparatus via the PVC, is unaffected, possibly suggesting that the primary membrane trafficking defects in the *erg2*Δ/Δ and *erg24*Δ/Δ mutants relate to the prevacuolar secretory pathway rather than to Golgi-to-vacuole or Golgi-to-plasma membrane transport. Our recent finding that a *C. albicans vps21*Δ/Δ mutant with defects in membrane trafficking through the PVC is hypersensitive to the morpholine antifungals provides further evidence of a functional interaction between Erg2p and Erg24p activities and trafficking through this organelle (3). It is also consistent with studies of *S. cerevisiae*, in which it has been shown that the transport of various proteins to the plasma membrane and their maintenance at the membrane, as well as their endocytic transport through the PVC on the way to the vacuole for degradation, are affected by the availability of ergosterol (4, 58, 59).

Given their reduced growth rates, deficiencies in stress tolerance, reduced protease secretion, and impaired hyphal growth, we were anticipating that both the *erg2*Δ/Δ and *erg24*Δ/Δ mutants would be avirulent *in vivo*. This was further supported by the study of Jia et al. (34), who reported that their *erg24*Δ/Δ mutant caused substantially less mortality than the control in a mouse model of disseminated candidiasis. Accordingly, we found that both the *erg2*Δ/Δ and *erg24*Δ/Δ mutants were essentially avirulent in the mouse model of disseminated candidiasis. However, both mutants efficiently colonized mouse vaginal tissue, with CFU counts exceeding those of the isogenic control strains. While it is possible that the CFU counts for the mutant strains were artificially elevated due to their limited capacity to elaborate multicellular hyphal forms, this result is nonetheless surprising. While the magnitude of the host response as determined by PMN counts was lower than that of the control strains, our data suggest that either mutant may be competent to cause a symptomatic infection. Others have noted that mutants with virulence defects in the mouse disseminated model are apparently able to survive and colonize the mouse vagina (60). This perhaps reflects the exquisite adaptation of *C. albicans* for survival upon the mucosal surface of the reproductive tract of mammals, and as such, this may be an environment that imposes little stress upon this fungus. Either way, these data suggest that ergosterol is less important for *C. albicans* survival within the vaginal environment. Thus, while targeting either the Erg2p or Erg24p enzyme could provide potentially efficacious therapies for treating disseminated fungal infections, these enzymes may not provide viable targets for treating vaginal candidiasis. Notably, the Erg24p enzyme acts immediately downstream of lanosterol demethylase, the target of fluconazole, which remains the preferred treatment for vaginal candidiasis (61). Put in the context of the often recurrent nature of vaginal candidiasis (62), it may be important to ask if targeting ergosterol biosynthesis is an optimal strategy for treating women with recurrent vaginal candidiasis. Despite this, some yeast mutants lacking nonessential enzymes within the ergosterol biosynthetic pathway are highly susceptible to a wide variety of xenobiotics (63). This was exemplified by the susceptibility of the *C. albicans erg2*Δ/Δ and *erg24*Δ/Δ mutants to terbinafine, vanadate, and rapamycin in this study and is most likely due to the increased fluidity and permeability of the mutant plasma membranes. Thus, while drugs that specifically target either Erg2p or Erg24p may not by themselves result in the preferred fungicidal outcome, they are likely to reduce the inherent virulence of the invading fungal pathogen and may greatly enhance the susceptibility of the pathogen to a wide range of antimicrobial compounds. Furthermore, as exemplified by the morpholine antifungals, drugs that simultaneously inhibit multiple steps of ergosterol biosynthesis may have greatly improved efficacy. As such, drugs that target either Erg2p or Erg24p may have great potential as adjunctive therapies.

ACKNOWLEDGMENTS

Research reported in this publication was supported by the National Institute of Allergy and Infectious Diseases of the National Institutes of Health (award numbers R21AI097664 and R01AI099080).

The content of this study is solely the responsibility of the authors and does not necessarily represent the official views of the National Institutes of Health.

We thank Aaron Mitchell (Carnegie Mellon University) and William Fonzi (Georgetown University) for providing strains and plasmids that were used in this study. Some images presented were acquired with the assistance of the LSU Health Sciences Center Morphology and Imaging Core. Finally, we also thank Promega Corporation for permission to produce and utilize the *C. albicans*-adapted Nluc coding sequence.

REFERENCES

1. **Odds FC, Brown AJ, Gow NA.** 2003. Antifungal agents: mechanisms of action. Trends Microbiol **11:**272–279. http://dx.doi.org/10.1016/S0966-842X(03)00117-3.
2. **Kelly SL, Lamb DC, Corran AJ, Baldwin BC, Kelly DE.** 1995. Mode of action and resistance to azole antifungals associated with the formation of 14 alpha-methylergosta-8,24(28)-dien-3beta,6alpha-diol. Biochem Biophys Res Commun **207:**910–915. http://dx.doi.org/10.1006/bbrc.1995.1272.
3. **Luna-Tapia A, Kerns ME, Eberle KE, Jursic BS, Palmer GE.** 2015. Trafficking through the late endosome significantly impacts *Candida albicans* tolerance of the azole antifungals. Antimicrob Agents Chemother **59:**2410–2420. http://dx.doi.org/10.1128/AAC.04239-14.
4. **Heese-Peck A, Pichler H, Zanolari B, Watanabe R, Daum G, Riezman H.** 2002. Multiple functions of sterols in yeast endocytosis. Mol Biol Cell **13:**2664–2680. http://dx.doi.org/10.1091/mbc.E02-04-0186.
5. **Kato M, Wickner WT.** 2001. Ergosterol is required for the Sec18/ATP-dependent priming step of homotypic vacuole fusion. EMBO J **20:**4035–4040. http://dx.doi.org/10.1093/emboj/20.15.4035.
6. **Seeley ES, Kato M, Margolis N, Wickner W, Eitzen G.** 2002. Genomic analysis of homotypic vacuole fusion. Mol Biol Cell **13:**782–794. http://dx.doi.org/10.1091/mbc.01-10-0512.
7. **Zhang YQ, Gamarra S, Garcia-Effron G, Park S, Perlin DS, Rao R.** 2010. Requirement for ergosterol in V-ATPase function underlies antifungal activity of azole drugs. PLoS Pathog **6:**e1000939. http://dx.doi.org/10.1371/journal.ppat.1000939.
8. **Johnston DA, Eberle KE, Sturtevant JE, Palmer GE.** 2009. Role for endosomal and vacuolar GTPases in *Candida albicans* pathogenesis. Infect Immun **77:**2343–2355. http://dx.doi.org/10.1128/IAI.01458-08.
9. **Palmer GE.** 2010. Endosomal and AP-3-dependent vacuolar trafficking routes make additive contributions to *Candida albicans* hyphal growth and pathogenesis. Eukaryot Cell **9:**1755–1765. http://dx.doi.org/10.1128/EC.00029-10.
10. **Palmer GE, Kelly MN, Sturtevant JE.** 2005. The *Candida albicans* vacuole is required for differentiation and efficient macrophage killing. Eukaryot Cell **4:**1677–1686. http://dx.doi.org/10.1128/EC.4.10.1677-1686.2005.
11. **Patenaude C, Zhang Y, Cormack B, Kohler J, Rao R.** 2013. Essential role for vacuolar acidification in *Candida albicans* virulence. J Biol Chem **288:**26256–26264. http://dx.doi.org/10.1074/jbc.M113.494815.
12. **Poltermann S, Nguyen M, Gunther J, Wendland J, Hartl A, Kunkel W, Zipfel PF, Eck R.** 2005. The putative vacuolar ATPase subunit Vma7p of *Candida albicans* is involved in vacuole acidification, hyphal development and virulence. Microbiology **151:**1645–1655. http://dx.doi.org/10.1099/mic.0.27505-0.
13. **Rane HS, Bernardo SM, Raines SM, Binder JL, Parra KJ, Lee SA.** 2013. *Candida albicans VMA3* is necessary for V-ATPase assembly and function and contributes to secretion and filamentation. Eukaryot Cell **12:**1369–1382. http://dx.doi.org/10.1128/EC.00118-13.
14. **Cornet M, Gaillardin C, Richard ML.** 2006. Deletions of the endocytic components *VPS28* and *VPS32* in *Candida albicans* lead to echinocandin and azole hypersensitivity. Antimicrob Agents Chemother **50:**3492–3495. http://dx.doi.org/10.1128/AAC.00391-06.
15. **Liu Y, Solis NV, Heilmann CJ, Phan QT, Mitchell AP, Klis FM, Filler SG.** 2014. Role of retrograde trafficking in stress response, host cell interactions, and virulence of *Candida albicans*. Eukaryot Cell **13:**279–287. http://dx.doi.org/10.1128/EC.00295-13.
16. **Barrett-Bee K, Dixon G.** 1995. Ergosterol biosynthesis inhibition: a target for antifungal agents. Acta Biochim Pol **42:**465–479.
17. **Burke D, Dawson D, Stearns T, Cold Spring Harbor Laboratory.** 2000. Methods in yeast genetics: a Cold Spring Harbor Laboratory course manual. Cold Spring Harbor Laboratory Press, Cold Spring Harbor, NY.
18. **Ramon AM, Fonzi WA.** 2003. Diverged binding specificity of Rim101p, the *Candida albicans* ortholog of PacC. Eukaryot Cell **2:**718–728. http://dx.doi.org/10.1128/EC.2.4.718-728.2003.
19. **Johnston DA, Luna-Tapia A, Eberle KE, Palmer GE.** 2013. Three prevacuolar compartment Rab GTPases impact *Candida albicans* hyphal growth. Eukaryot Cell **12:**1039–1050. http://dx.doi.org/10.1128/EC.00359-12.
20. **Hall MP, Unch J, Binkowski BF, Valley MP, Butler BL, Wood MG, Otto P, Zimmerman K, Vidugiris G, Machleidt T, Robers MB, Benink HA, Eggers CT, Slater MR, Meisenheimer PL, Klaubert DH, Fan F, Encell LP, Wood KV.** 2012. Engineered luciferase reporter from a deep sea shrimp utilizing a novel imidazopyrazinone substrate. ACS Chem Biol **7:**1848–1857. http://dx.doi.org/10.1021/cb3002478.
21. **Mukhtar M, Logan DA, Kaufer NF.** 1992. The carboxypeptidase Y-encoding gene from *Candida albicans* and its transcription during yeast-to-hyphae conversion. Gene **121:**173–177. http://dx.doi.org/10.1016/0378-1119(92)90178-R.
22. **Gillum AM, Tsay EY, Kirsch DR.** 1984. Isolation of the *Candida albicans* gene for orotidine-5′-phosphate decarboxylase by complementation of *S. cerevisiae ura3* and *E. coli pyrF* mutations. Mol Gen Genet **198:**179–182. http://dx.doi.org/10.1007/BF00328721.
23. **Fonzi WA, Irwin MY.** 1993. Isogenic strain construction and gene mapping in *Candida albicans*. Genetics **134:**717–728.
24. **Gietz D, St Jean A, Woods RA, Schiestl RH.** 1992. Improved method for high efficiency transformation of intact yeast cells. Nucleic Acids Res **20:**1425. http://dx.doi.org/10.1093/nar/20.6.1425.
25. **Wilson RB, Davis D, Mitchell AP.** 1999. Rapid hypothesis testing with *Candida albicans* through gene disruption with short homology regions. J Bacteriol **181:**1868–1874.
26. **Lay J, Henry LK, Clifford J, Koltin Y, Bulawa CE, Becker JM.** 1998. Altered expression of selectable marker *URA3* in gene-disrupted *Candida albicans* strains complicates interpretation of virulence studies. Infect Immun **66:**5301–5306.
27. **Crandall M, Edwards JE, Jr.** 1987. Segregation of proteinase-negative mutants from heterozygous *Candida albicans*. J Gen Microbiol **133:**2817–2824.
28. **Palmer GE, Sturtevant JE.** 2004. Random mutagenesis of an essential *Candida albicans* gene. Curr Genet **46:**343–356. http://dx.doi.org/10.1007/s00294-004-0538-0.
29. **Brown DH, Jr, Giusani AD, Chen X, Kumamoto CA.** 1999. Filamentous growth of *Candida albicans* in response to physical environmental cues and its regulation by the unique *CZF1* gene. Mol Microbiol **34:**651–662. http://dx.doi.org/10.1046/j.1365-2958.1999.01619.x.
30. **Vida TA, Emr SD.** 1995. A new vital stain for visualizing vacuolar membrane dynamics and endocytosis in yeast. J Cell Biol **128:**779–792. http://dx.doi.org/10.1083/jcb.128.5.779.
31. **Baggett JJ, Shaw JD, Sciambi CJ, Watson HA, Wendland B.** 2003. Fluorescent labeling of yeast. Curr Protoc Cell Biol **Chapter 4:**Unit 4.13. http://dx.doi.org/10.1002/0471143030.cb0413s20.
32. **Peters BM, Palmer GE, Nash AK, Lilly EA, Fidel PL, Jr, Noverr MC.** 2014. Fungal morphogenetic pathways are required for the hallmark inflammatory response during *Candida albicans* vaginitis. Infect Immun **82:**532–543. http://dx.doi.org/10.1128/IAI.01417-13.
33. **Donegan K, Matyac C, Seidler R, Porteous A.** 1991. Evaluation of methods for sampling, recovery, and enumeration of bacteria applied to the phylloplane. Appl Environ Microbiol **57:**51–56.
34. **Jia N, Arthington-Skaggs B, Lee W, Pierson CA, Lees ND, Eckstein J, Barbuch R, Bard M.** 2002. Candida albicans sterol C-14 reductase, encoded by the *ERG24* gene, as a potential antifungal target site. Antimicrob Agents Chemother **46:**947–957. http://dx.doi.org/10.1128/AAC.46.4.947-957.2002.
35. **Shah Alam Bhuiyan M, Eckstein J, Barbuch R, Bard M.** 2007. Synthetically lethal interactions involving loss of the yeast *ERG24*: the sterol C-14 reductase gene. Lipids **42:**69–76. http://dx.doi.org/10.1007/s11745-006-1001-4.
36. **Baloch RI, Mercer EI, Wiggins TE, Baldwin BC.** 1984. Inhibition of ergosterol biosynthesis in *Saccharomyces cerevisiae* and *Ustilago maydis* by tridemorph, fenpropimorph and fenpropidin. Phytochemistry **23:**2219–2226. http://dx.doi.org/10.1016/S0031-9422(00)80523-3.
37. **Klionsky DJ, Herman PK, Emr SD.** 1990. The fungal vacuole: composition, function, and biogenesis. Microbiol Rev **54:**266–292.
38. **Palmer GE, Cashmore A, Sturtevant J.** 2003. Candida albicans VPS11 is required for vacuole biogenesis and germ tube formation. Eukaryot Cell **2:**411–421. http://dx.doi.org/10.1128/EC.2.3.411-421.2003.

39. **Kane PM.** 2007. The long physiological reach of the yeast vacuolar H+-ATPase. J Bioenerg Biomembr **39:**415–421. http://dx.doi.org/10.1007/s10863-007-9112-z.
40. **Raymond CK, Howald-Stevenson I, Vater CA, Stevens TH.** 1992. Morphological classification of the yeast vacuolar protein sorting mutants: evidence for a prevacuolar compartment in class E *vps* mutants. Mol Biol Cell **3:**1389–1402. http://dx.doi.org/10.1091/mbc.3.12.1389.
41. **Valls LA, Hunter CP, Rothman JH, Stevens TH.** 1987. Protein sorting in yeast: the localization determinant of yeast vacuolar carboxypeptidase Y resides in the propeptide. Cell **48:**887–897. http://dx.doi.org/10.1016/0092-8674(87)90085-7.
42. **Valls LA, Winther JR, Stevens TH.** 1990. Yeast carboxypeptidase Y vacuolar targeting signal is defined by four propeptide amino acids. J Cell Biol **111:**361–368. http://dx.doi.org/10.1083/jcb.111.2.361.
43. **Bankaitis VA, Johnson LM, Emr SD.** 1986. Isolation of yeast mutants defective in protein targeting to the vacuole. Proc Natl Acad Sci U S A **83:**9075–9079. http://dx.doi.org/10.1073/pnas.83.23.9075.
44. **Rothman JH, Stevens TH.** 1986. Protein sorting in yeast: mutants defective in vacuole biogenesis mislocalize vacuolar proteins into the late secretory pathway. Cell **47:**1041–1051. http://dx.doi.org/10.1016/0092-8674(86)90819-6.
45. **Barelle CJ, Bohula EA, Kron SJ, Wessels D, Soll DR, Schafer A, Brown AJ, Gow NA.** 2003. Asynchronous cell cycle and asymmetric vacuolar inheritance in true hyphae of *Candida albicans*. Eukaryot Cell **2:**398–410. http://dx.doi.org/10.1128/EC.2.3.398-410.2003.
46. **Gow NA, Gooday GW.** 1982. Vacuolation, branch production and linear growth of germ tubes in *Candida albicans*. J Gen Microbiol **128:**2195–2198.
47. **Lo HJ, Kohler JR, DiDomenico B, Loebenberg D, Cacciapuoti A, Fink GR.** 1997. Nonfilamentous *C. albicans* mutants are avirulent. Cell **90:**939–949. http://dx.doi.org/10.1016/S0092-8674(00)80358-X.
48. **Saville SP, Lazzell AL, Monteagudo C, Lopez-Ribot JL.** 2003. Engineered control of cell morphology in vivo reveals distinct roles for yeast and filamentous forms of *Candida albicans* during infection. Eukaryot Cell **2:**1053–1060. http://dx.doi.org/10.1128/EC.2.5.1053-1060.2003.
49. **Carlisle PL, Banerjee M, Lazzell A, Monteagudo C, Lopez-Ribot JL, Kadosh D.** 2009. Expression levels of a filament-specific transcriptional regulator are sufficient to determine *Candida albicans* morphology and virulence. Proc Natl Acad Sci U S A **106:**599–604. http://dx.doi.org/10.1073/pnas.0804061106.
50. **Fidel PL, Jr, Barousse M, Espinosa T, Ficarra M, Sturtevant J, Martin DH, Quayle AJ, Dunlap K.** 2004. An intravaginal live *Candida* challenge in humans leads to new hypotheses for the immunopathogenesis of vulvovaginal candidiasis. Infect Immun **72:**2939–2946. http://dx.doi.org/10.1128/IAI.72.5.2939-2946.2004.
51. **Zinser E, Paltauf F, Daum G.** 1993. Sterol composition of yeast organelle membranes and subcellular distribution of enzymes involved in sterol metabolism. J Bacteriol **175:**2853–2858.
52. **Zinser E, Sperka-Gottlieb CD, Fasch EV, Kohlwein SD, Paltauf F, Daum G.** 1991. Phospholipid synthesis and lipid composition of subcellular membranes in the unicellular eukaryote *Saccharomyces cerevisiae*. J Bacteriol **173:**2026–2034.
53. **Lai MH, Bard M, Pierson CA, Alexander JF, Goebl M, Carter GT, Kirsch DR.** 1994. The identification of a gene family in the *Saccharomyces cerevisiae* ergosterol biosynthesis pathway. Gene **140:**41–49. http://dx.doi.org/10.1016/0378-1119(94)90728-5.
54. **Dupre S, Haguenauer-Tsapis R.** 2003. Raft partitioning of the yeast uracil permease during trafficking along the endocytic pathway. Traffic **4:**83–96. http://dx.doi.org/10.1034/j.1600-0854.2003.40204.x.
55. **Lauwers E, Andre B.** 2006. Association of yeast transporters with detergent-resistant membranes correlates with their cell-surface location. Traffic **7:**1045–1059. http://dx.doi.org/10.1111/j.1600-0854.2006.00445.x.
56. **Wiederhold E, Gandhi T, Permentier HP, Breitling R, Poolman B, Slotboom DJ.** 2009. The yeast vacuolar membrane proteome. Mol Cell Proteomics **8:**380–392. http://dx.doi.org/10.1074/mcp.M800372-MCP200.
57. **Lee SA, Jones J, Hardison S, Kot J, Khalique Z, Bernardo SM, Lazzell A, Monteagudo C, Lopez-Ribot J.** 2009. Candida albicans VPS4 is required for secretion of aspartyl proteases and in vivo virulence. Mycopathologia **167:**55–63. http://dx.doi.org/10.1007/s11046-008-9155-7.
58. **Bagnat M, Chang A, Simons K.** 2001. Plasma membrane proton ATPase Pma1p requires raft association for surface delivery in yeast. Mol Biol Cell **12:**4129–4138. http://dx.doi.org/10.1091/mbc.12.12.4129.
59. **Daicho K, Makino N, Hiraki T, Ueno M, Uritani M, Abe F, Ushimaru T.** 2009. Sorting defects of the tryptophan permease Tat2 in an erg2 yeast mutant. FEMS Microbiol Lett **298:**218–227. http://dx.doi.org/10.1111/j.1574-6968.2009.01722.x.
60. **Rane HS, Hardison S, Botelho C, Bernardo SM, Wormley F, Jr, Lee SA.** 2014. *Candida albicans VPS4* contributes differentially to epithelial and mucosal pathogenesis. Virulence **5:**810–818. http://dx.doi.org/10.4161/21505594.2014.956648.
61. **Sobel JD.** 2013. Factors involved in patient choice of oral or vaginal treatment for vulvovaginal candidiasis. Patient Prefer Adherence **8:**31–34. http://dx.doi.org/10.2147/PPA.S38984.
62. **Foxman B, Muraglia R, Dietz JP, Sobel JD, Wagner J.** 2013. Prevalence of recurrent vulvovaginal candidiasis in 5 European countries and the United States: results from an Internet panel survey. J Low Genit Tract Dis **17:**340–345. http://dx.doi.org/10.1097/LGT.0b013e318273e8cf.
63. **Jensen-Pergakes KL, Kennedy MA, Lees ND, Barbuch R, Koegel C, Bard M.** 1998. Sequencing, disruption, and characterization of the *Candida albicans* sterol methyltransferase (*ERG6*) gene: drug susceptibility studies in *erg6* mutants. Antimicrob Agents Chemother **42:**1160–1167.